

Scanning-tunneling-microscopy study of Pb on Si(111)

D. Tang and H. E. Elsayed-Ali

Physical Electronics Research Institute, Department of Electrical and Computer Engineering, Old Dominion University, Norfolk, Virginia 23529

J. Wendelken and J. Xu

Oak Ridge National Laboratory, Oak Ridge, Tennessee 37831

(Received 23 March 1995)

Scanning-tunneling microscopy has been used to study temperature and coverage dependence of the structure of lead on the Si(111)- 7×7 surface. For low Pb coverage, the Pb atoms favored the faulted sites. The ratio between the number of Pb atoms on faulted to unfaulted sites increased after sample annealing. An energy difference of 0.05 eV associated with a Pb atom on these two sites is estimated. The mobility of Pb atoms on Si(111) was observed at a temperature as low as 260 °C for a coverage of 0.1 and 1 ML.

Lead on silicon represents an attractive system to study metal-semiconductor interfaces. Phase diagrams do not show the presence of any chemical compounds at the Pb/Si interface. Only for such well-defined metal-semiconductor contacts will it be possible to relate their electronic properties directly to the crystal structure and chemical binding at the interface. Mutual solubilities of Pb in Si are negligibly small,¹ thus the interface is abrupt. These properties make the Pb/Si interface a good system for studying the basic interactions of metals on semiconductors.

Several studies have been done on the Pb/Si(111) interface.²⁻⁸ These studies have utilized a variety of surface analysis techniques including low-energy electron diffraction (LEED), scanning tunneling microscopy (STM), low-energy ion-scattering spectroscopy, Auger-electron spectroscopy, reflection high-energy electron diffraction, photoemission spectroscopy, and thermal desorption. In contrast to the above-mentioned chemical simplicity of the Pb/Si interaction, a relatively complex surface structural behavior was observed. For example, three different $\sqrt{3}\times\sqrt{3}$ phases were reported by Le Lay *et al.*¹ In addition, the final Pb structure on the Si(111) depends on the annealing history³ as well as deposition rate and substrate temperature. Thus, more investigations are necessary for better understanding of the structural properties of the Pb/Si interface. Here we report on a temperature-dependent STM study of the Pb/Si(111) interface. At a coverage less than ~ 0.1 monolayer, the Pb atoms appear to favor the faulted sites on the Si(111)- 7×7 unit cell. We measured the ratio between the number of occupied faulted and unfaulted sites after proper annealing. Based on that measurement, we can calculate the energy difference associated with Pb atoms on the two different sites.

Our experiments were performed in an ultrahigh vacuum chamber, equipped with both STM and LEED facilities. The base pressure of the chamber was $\sim 1\times 10^{-10}$ torr. The Si(111) samples used in these measurements were cut from a *p*-type wafer with 1 Ω cm resistivity, and had a size of $10\times 3\times 0.2$ mm³. The samples were

clamped on a tantalum mounting stage. Lead was evaporated from a cell at 570 °C. The silicon samples were heated resistively by directly passing current through them. Each new sample was outgassed by heating it overnight at 600 °C. Samples were cleaned with several flashes up to 1250 °C, followed by annealing at 900 °C for 0.5 min. and then slow cooling at a rate of about 0.5 °C/sec. The sample temperature was measured by two pyrometers, to cover a temperature range of 200–1250 °C, and the sample cleanliness was monitored by observation of the sharp 7×7 LEED pattern as well as STM images. Figure 1 shows a typical STM image of a clean Si(111)- 7×7 surface structure. A single-atom step is also shown in the image.

Growth experiments were performed at room temperature for a coverage range of $0\leq\theta\leq 3$ ML where a monolayer is defined as 7.85×10^{14} atoms/cm². Figure 2 shows

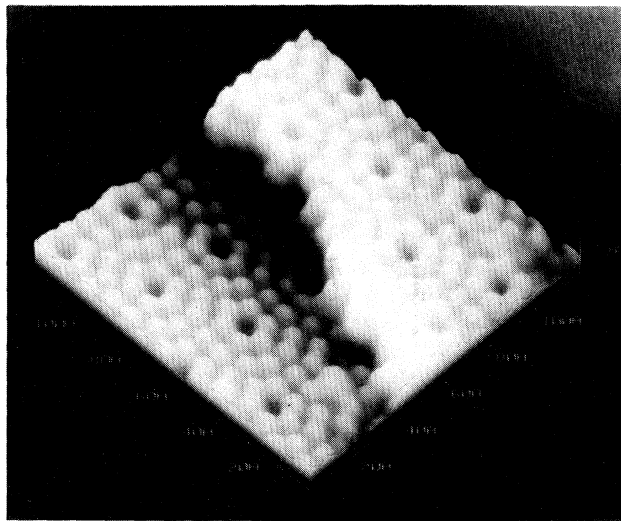


FIG. 1. An STM image of a clean Si(111)- 7×7 with a step on it. The image size is 110×110 Å², obtained at sample bias of 2 V and 0.7 nA constant tunneling current.

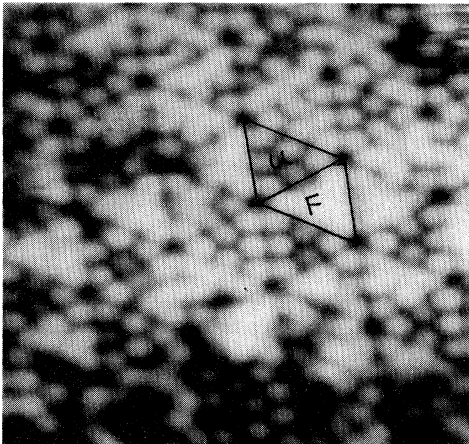


FIG. 2. A $140 \times 140 \text{ \AA}^2$ STM image of 0.07 ML Pb on Si(111)- 7×7 at room temperature. Trios of Pb atoms are preferentially covering the faulted side of the 7×7 unit cell. The STM was operated at 0.2 nA constant tunneling current, with 0.4 V bias on the sample.

an STM image of 0.07 ML Pb on Si(111)- 7×7 . For this coverage, the Si(111)- 7×7 LEED pattern did not change significantly from its original shape. Our results show that the Pb atoms favored the faulted sites in the unit cell of the 7×7 structure and formed trios. This is consistent with a previous STM measurement.³ Similar behavior was found in the Ag/Si(111)- 7×7 (Refs. 9 and 10) and the Pd/Si(111)- 7×7 (Ref. 11) systems. For the Si(111)- 7×7 structure, the Si-atom-induced surface states are mainly derived from the interaction between the adatom P orbital and the dangling-bond orbital of the Si bilayer. Tunneling current spectroscopic images of these adatom dangling-bond states suggest a significantly higher state density for the adatom on the faulted site than on the unfaulted site of the unit cell.¹² In the dimer-adatom-stacking-fault model,¹³ the Si lattice on the unfaulted side has an atom in the second bilayer sitting directly in the middle of a ring of six atoms making up the first bilayer. This leads to a fairly closed structure. In contrast, on the faulted half, the first bilayer is rotated 180° to line up with the second bilayer. This openness may explain why faulted sites are preferred by the Pb atoms.¹¹

We next heated the sample and observed the distribution of Pb atoms in relation to the faulted and unfaulted Si(111)- 7×7 sites. After annealing at 260°C for 40 sec, more Pb atoms are observed on the faulted sites, causing the ratio R of Pb at faulted sites to that at unfaulted sites to increase. The high mobility of Pb atoms on the surface implies that Pb atoms overcome the relatively small energy barriers which inhibit Pb atoms from diffusion on the Si substrate. It is possible to estimate the energy difference ΔE associated with the Pb atoms at faulted and unfaulted sites, using the ratio R after annealing,

$$R = \frac{N_f}{N_u} = e^{(-\Delta E/KT)},$$

where N_f and N_u are numbers of faulted and unfaulted

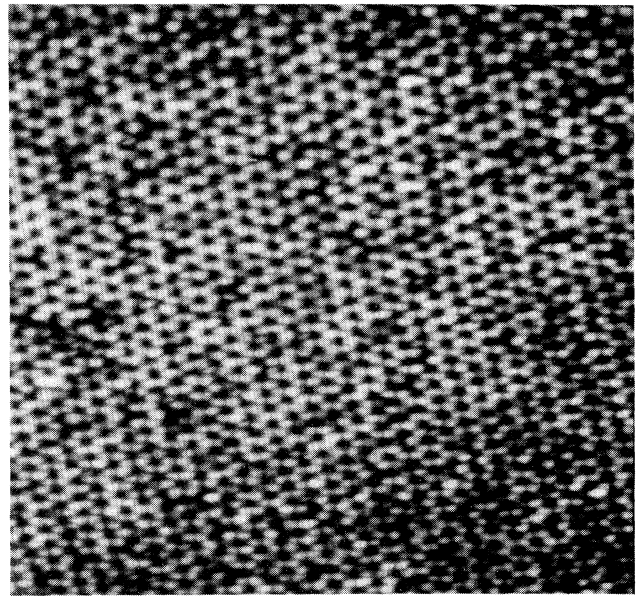


FIG. 3. A $750 \times 800 \text{ \AA}^2$ STM image of 0.3 ML Pb on Si(111)- 7×7 at room temperature. The STM was operated at 0.2 nA constant tunneling current, with 1.5 V bias on the sample.

sites occupied by Pb atoms, respectively, K is Boltzmann's constant, and T is the surface temperature. This ratio R is about 2.5 in our case. An increase in R when annealing the sample was also observed for the Ag/Si(111)- 7×7 system.¹⁰

We believe that the mechanism for the increase of the ratio R with annealing is not solely due to the thermal statistics. There are 19 dangling bonds on every Si(111)- 7×7 unit, 18 of them in faulted and unfaulted sites, and none of them in the dimer walls. At low coverage, Pb atoms bond first at the dangling bonds; this can be seen from Fig. 3, which shows an STM image of 0.3 ML Pb on

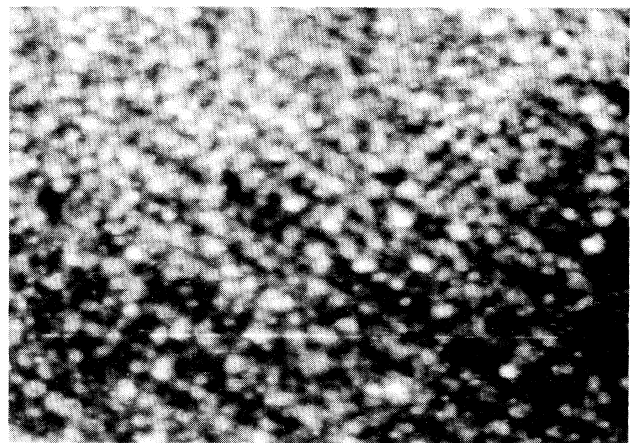


FIG. 4. An $800 \times 600 \text{ \AA}^2$ STM image of 1 ML Pb deposited on Si(111)- 7×7 at room temperature deposition. No annealing was performed. The STM was operated at 0.2 nA constant tunneling current, with 0.5 V bias on the sample.

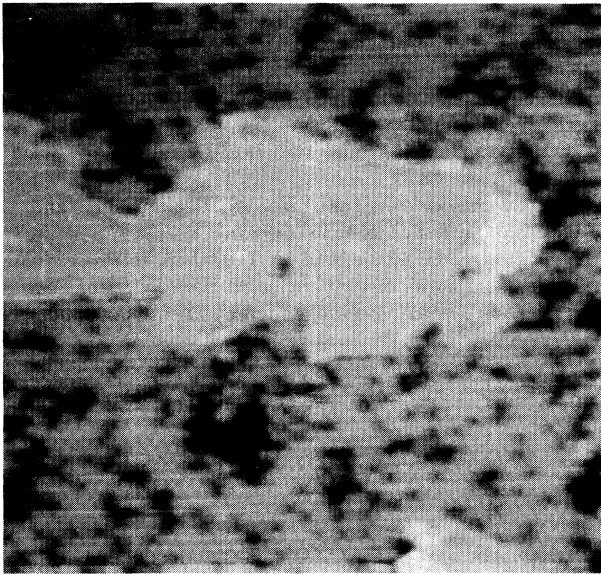


FIG. 5. A $360 \times 390 \text{ \AA}^2$ STM image of 1 ML Pb deposited on Si(111)- 7×7 at room temperature then annealed at 260°C for 30 sec. The area is covered by 1×1 and $\sqrt{3} \times \sqrt{3}$ domains. The STM was operated at 0.2 nA constant tunneling current, with 1.5 V bias on the sample.

Si(111)- 7×7 ; the dimer walls are still clear at this coverage. This implies that the energy barriers on the dimer walls are higher than the energy difference between the faulted and unfaulted sites. Proper annealing makes Pb atoms gain enough energy to overcome the barrier; the resulting Pb atom distribution on faulted and unfaulted sites could reflect the energy difference. From the value of the ratio R , we estimate that this energy difference ΔE is ~ 0.05 eV. It is likely that this energy difference is affected by the formation of the stacking fault in the Si(111)- 7×7 unit cell. The stacking fault introduces a new state with an energy of 0.1 eV on top of the valence band at Γ .¹⁴ In addition, theoretical calculations have found that the introduction of a stacking fault into the top layer raises the surface energy slightly, in the range 0.02–0.06 eV per 1×1 cell.¹⁵ This is similar to the energy cost of a stacking fault in the bulk, which has been calculated to be ~ 0.04 eV per 1×1 cell.¹⁶

We next consider higher coverage of Pb on the Si(111). Figure 4 shows an STM image of 1 ML of Pb deposited at room temperature. The growth of Pb on Si(111)- 7×7 was observed to follow the Stranski-Krastanov (layer-plus-island) growth mechanism; however, the intermediate layers have a different structure and formation process at different deposition temperatures. At room temperature, the intermediate layer was found to be a Pb(111) epitaxial layer with the Pb[110] direction parallel to the Si[110] direction. The intermediate Pb(111) layer,

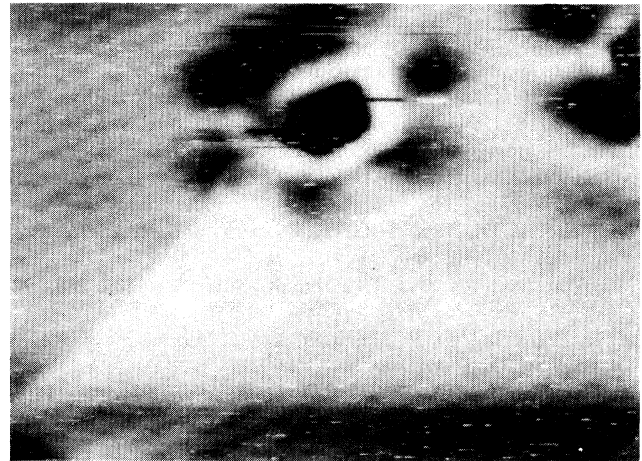


FIG. 6. A $90 \times 75 \text{ \AA}^2$ STM image of 1×1 structure in Fig. 5. The STM was operated at 0.3 nA constant tunneling current, with 1.5 V bias on the sample.

which is not observed by STM, is possibly shrunk by up to 5.3% for lattice matching.⁴ We also observed that the Pb atoms were mobile at a coverage of 1 ML after annealing the sample at 260°C for 40 sec. After such annealing, the LEED pattern was observed to change with new spots corresponding to the $\sqrt{3} \times \sqrt{3}$ structure, rotated 30° . Meanwhile, the STM image after annealing shows that the Pb atoms formed a mixture of islands with 1×1 and $\sqrt{3} \times \sqrt{3}$ structures appearing. Figure 5 is an example of this mixture of 1×1 and $\sqrt{3} \times \sqrt{3}$ $R 30^\circ$ structures. As in previous measurements, using the same sample voltage bias, we cannot distinguish atoms of 1×1 and $\sqrt{3} \times \sqrt{3}$ structures.³ In Fig. 6 we show the 1×1 structure in which atoms could not be distinguished in Fig. 5. This 1×1 structure is not a compressed Pb(111) overlayer after annealing, though its [110] direction is still parallel to the Si[110] direction. The spacing of the Pb atoms is $\sim 3.5 \text{ \AA}$, which is equivalent to a coverage of 1.2 ML as defined before. Meanwhile, our $\sqrt{3} \times \sqrt{3}$ structure is equivalent to $\frac{1}{3}$ ML Pb coverage. This kind of 1×1 structure is different from that previously observed for Pb deposition done at 340°C , which undergoes a reversible phase transition below $\sim 300^\circ\text{C}$ to a type of $\sqrt{3} \times \sqrt{3}$ $R 30^\circ$.¹

In conclusion, we have observed that Pb atoms are mobile on the Si(111) surface at a temperature of 260°C . The energy difference between the Pb faulted and unfaulted sites is estimated to be 0.05 eV. This energy is close to the theoretical calculation of energy induced by a stacking fault in the bulk.

This work was supported by the Southeastern Universities Research Association under the Oak Ridge Summer Cooperative Research Program and the U.S. Department of Energy, under Grant No. DE-FG05-93ER45504.

- ¹G. Le Lay, J. Peretti, M. Hanbucken, and W. S. Yang, *Surf. Sci.* **204**, 57 (1988).
- ²P. J. Estrup and J. Morrison, *Surf. Sci.* **2**, 465 (1964).
- ³E. Ganz, F. Xiong, I. Hwang, and J. Golovchenko, *Phys. Rev. B* **43**, 7316 (1991); E. Ganz, I. Hwang, F. Xiong, S. K. Theiss, and J. Golovchenko, *Surf. Sci.* **257**, 259 (1991).
- ⁴M. Saitoh, K. Oura, K. Asano, F. Shoji, and T. Hanawa, *Surf. Sci.* **154**, 394 (1985).
- ⁵L. Seehofer, D. Daboul, G. Falkenberg, and R. L. Johnson, *Surf. Sci.* **307-309**, 698 (1994).
- ⁶M. Wemmenhove and T. Hibman, *Surf. Sci.* **287/288**, 925 (1993).
- ⁷H. H. Weitering, D. R. Heslinga, and T. Hibma, *Phys. Rev. B* **45**, 5991 (1992).
- ⁸H. H. Weitering, A. R. H. F. Ettema, and T. Hibma, *Phys. Rev. B* **45**, 9126 (1992).
- ⁹S. Tosch and H. Neddermeyer, *Phys. Rev. Lett.* **61**, 349 (1988).
- ¹⁰A. Shibata, Y. Kimura, and K. Takayanagi, *Surf. Sci.* **303**, 161 (1994).
- ¹¹U. K. Köhler, J. E. Demuth, and R. J. Hamers, *Phys. Rev. Lett.* **60**, 2499 (1988).
- ¹²R. J. Hamers, R. M. Tromp, and J. E. Demuth, *Surf. Sci.* **181**, 346 (1987).
- ¹³K. Takayanagi, Y. Tanishiro, S. Takahashi, and M. Takahashi, *Surf. Sci.* **164**, 367 (1985).
- ¹⁴M. Y. Chou, S. G. Louie, and M. L. Cohen, in *Proceedings of the 17th International Conference on the Physics of Semiconductors, San Francisco, 1984*, edited by D. J. Chadi and W. A. Harrison (Springer, Berlin, 1985), pp. 43–46.
- ¹⁵R. D. Meade and D. Vanderbilt, *Phys. Rev. B* **40**, 3905 (1989).
- ¹⁶M. Y. Chou, M. L. Cohen, and S. G. Louie, *Phys. Rev. B* **32**, 7979 (1985).

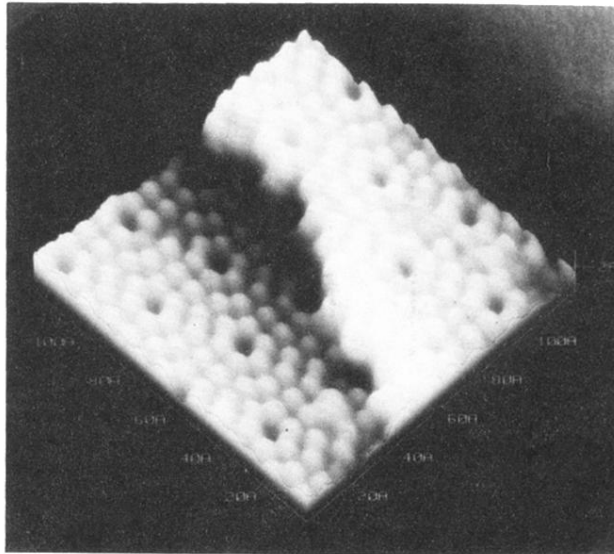


FIG. 1. An STM image of a clean Si(111)-7 \times 7 with a step on it. The image size is 110 \times 110 \AA^2 , obtained at sample bias of 2 V and 0.7 nA constant tunneling current.

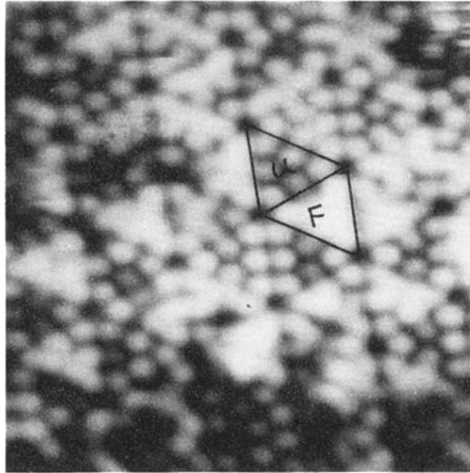


FIG. 2. A $140 \times 140 \text{ \AA}^2$ STM image of 0.07 ML Pb on Si(111)- 7×7 at room temperature. Trios of Pb atoms are preferentially covering the faulted side of the 7×7 unit cell. The STM was operated at 0.2 nA constant tunneling current, with 0.4 V bias on the sample.

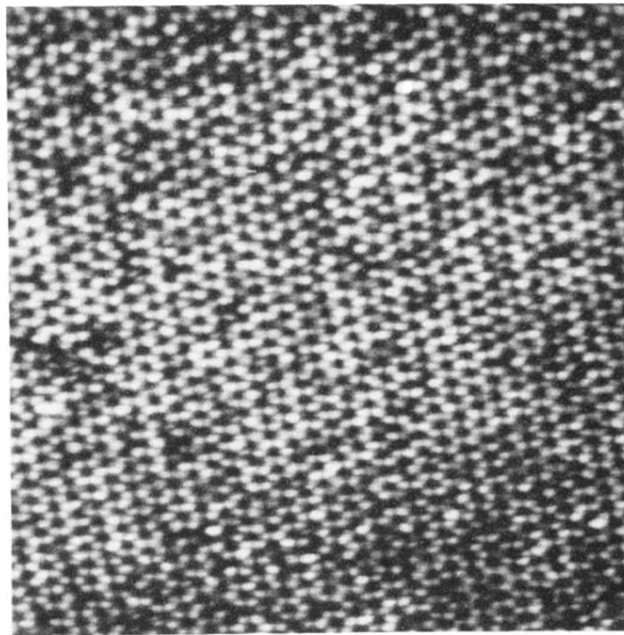


FIG. 3. A $750 \times 800 \text{ \AA}^2$ STM image of 0.3 ML Pb on Si(111)- 7×7 at room temperature. The STM was operated at 0.2 nA constant tunneling current, with 1.5 V bias on the sample.

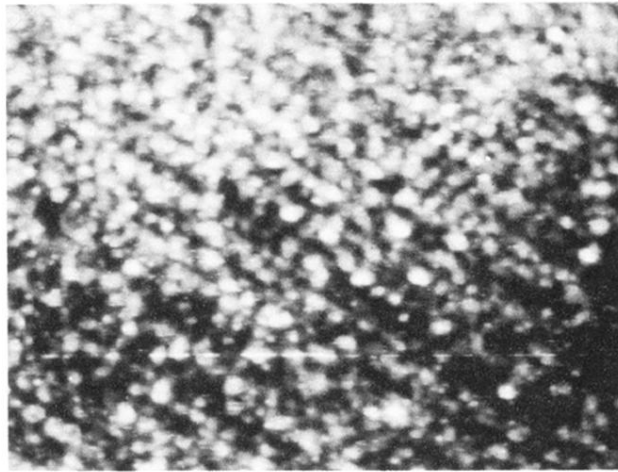


FIG. 4. An $800 \times 600 \text{ \AA}^2$ STM image of 1 ML Pb deposited on Si(111)- 7×7 at room temperature deposition. No annealing was performed. The STM was operated at 0.2 nA constant tunneling current, with 0.5 V bias on the sample.

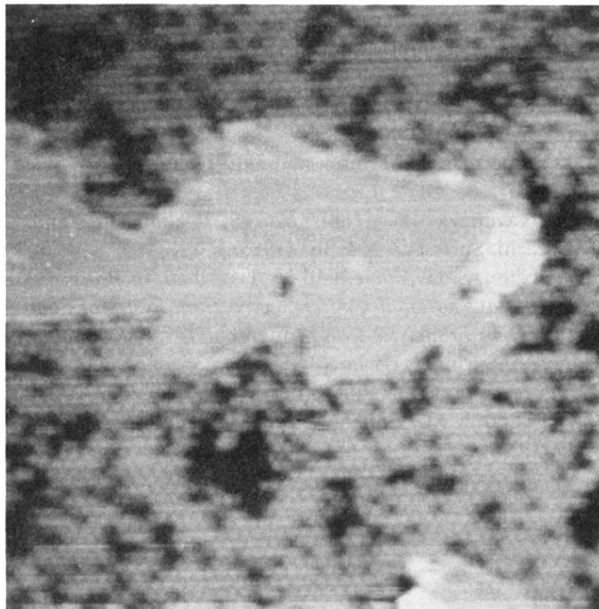


FIG. 5. A $360 \times 390 \text{ \AA}^2$ STM image of 1 ML Pb deposited on Si(111)- 7×7 at room temperature then annealed at 260°C for 30 sec. The area is covered by 1×1 and $\sqrt{3} \times \sqrt{3}$ domains. The STM was operated at 0.2 nA constant tunneling current, with 1.5 V bias on the sample.

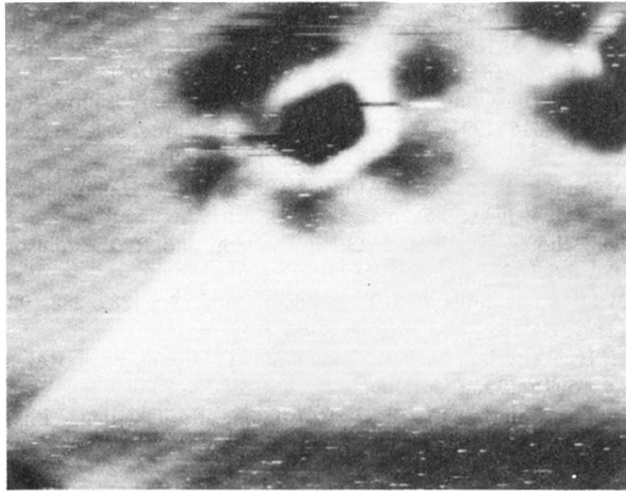


FIG. 6. A $90 \times 75 \text{ \AA}^2$ STM image of 1×1 structure in Fig. 5. The STM was operated at 0.3 nA constant tunneling current, with 1.5 V bias on the sample.